

Edge-type misfit dislocations produced by thermal processing of pre-relaxed $\text{In}_x\text{Ga}_{1-x}\text{As}/\text{GaAs}$ heterostructures

X. W. Liu and A. A. Hopgood^{a)}

The Open University, Faculty of Technology, Walton Hall, Milton Keynes, MK7 6AA, United Kingdom

B. F. Usher

La Trobe University, Department of Electronic Engineering, Bundoora, Victoria 3083, Australia

H. Wang

Nanyang Technological University, Microelectronics Centre, School of Electrical and Electronic Engineering, Singapore 639798

N. S. Braithwaite

The Open University, Faculty of Technology, Walton Hall, Milton Keynes, MK7 6AA, United Kingdom

(Received 11 April 2000; accepted for publication 14 August 2000)

Dislocation structures are presented for $\text{GaAs}/\text{In}_x\text{Ga}_{1-x}\text{As}/\text{GaAs}$ heterostructures before and after thermal processing. Cathodoluminescence has allowed nondestructive examination of bulk specimens, while transmission electron microscopy has been used to establish the details of the dislocation configurations. In each as-grown specimen the thickness of the $\text{In}_x\text{Ga}_{1-x}\text{As}$ layer was above its critical value, so 60° misfit dislocations were already present. It is shown that new pure edge, i.e., 90° , dislocations are formed at the interfaces by thermal processing at 1040 K. Their Burgers vectors are $a/2\langle 101 \rangle$ perpendicular to their $\langle 010 \rangle$ directions. Although individual 90° misfit dislocations are more effective relievers of strain than 60° ones, the self-energy for an array of such dislocations is higher and hence 60° misfit dislocations form first. A model of the formation of 90° edge misfit dislocations is proposed in which the climb of vacancy-producing jogs on pre-existing 60° dislocations leaves a trailing dislocation dipole. © 2000 American Institute of Physics. [S0021-8979(00)03822-6]

I. INTRODUCTION

Strained-layer semiconductor lasers have huge commercial significance for the telecommunications industry. The reliability of these devices is dependent on the stability of the strained layer, and hence on the propensity to form misfit dislocations at the strained-layer interfaces. In other applications, for instance where a misfitting layer is to be used as a buffer, complete relaxation of the layer is desired. In all cases, the ability to reliably predict the level of dislocation introduction and consequent strain relaxation is vital.

The accommodation of misfit between an epitaxial film and its substrate by misfit dislocations has been the subject of intensive investigation.^{1,2} In heteroepitaxial semiconductor systems with the zincblende structure, orthogonal arrays of 60° misfit dislocations at interfaces have been assumed to be the general means by which misfitting layers are relaxed.³ Most investigations of nucleation, propagation, and multiplication of misfit dislocations have been based on this premise, e.g., Refs. 4–6.

Beanland *et al.*⁷ have observed that the rotation of 60° dislocations into 90° dislocations produced additional misfit relief by the conversion of screw components into edge components. Preliminary observations of pure edge (i.e., 90°) misfit dislocations in heat-treated $\text{GaAs}/\text{In}_x\text{Ga}_{1-x}\text{As}/\text{GaAs}$,

where $x=0.15$, have previously been reported.⁸ In this article we extend those findings by considering both $x=0.15$ and $x=0.2$, and by complementing transmission electron microscopy (TEM) with cathodoluminescence (CL).

II. EXPERIMENTAL DETAILS

All the structures considered here comprise a single strained layer of $\text{In}_x\text{Ga}_{1-x}\text{As}$ between surrounding layers of GaAs. Two types of specimens were considered: $x=0.15$, $h=25$ nm and $x=0.20$, $h=20$ nm. In each case h exceeded the critical value for misfit dislocation formation, so the structures were already partially relaxed in their as-grown state.

The specimens were grown by molecular beam epitaxy. A 50 nm AlAs layer was first grown epitaxially on a GaAs (001) substrate, followed by a 200 nm layer of GaAs, a layer of $\text{In}_x\text{Ga}_{1-x}\text{As}$ of thickness h , and a second 200 nm layer of GaAs. The growth temperature was 800 K for the $\text{In}_x\text{Ga}_{1-x}\text{As}$ layer and 870 K for other layers. The growth rate was 1 $\mu\text{m}/\text{h}$. The composition and layer thickness were calibrated by x-ray diffraction. The surface morphology was monitored during growth by reflection high-energy electron diffraction.

The bulk specimens (~ 5 mm \times 5 mm) were annealed in a nitrogen atmosphere within a Carbolite furnace. The specimens were plunged into the furnace and, once the target temperature had been attained, were held there for 300 s

^{a)}Electronic mail: A.A.Hopgood@open.ac.uk, author to whom all correspondence should be addressed.

before being withdrawn from the furnace to cool. Specimens were annealed in pairs, placed face-to-face in order to reduce the possibility of arsenic atoms escaping from the surfaces. Subsequent CL and TEM imaging showed that no surface damage had occurred.

CL on a JEOL JSM-820 scanning electron microscope allowed dislocations to be examined at low magnification in a bulk specimen, thereby avoiding the risk of dislocation configuration being altered by specimen preparation. Film specimens for TEM observation were prepared using the epitaxial lift-off technique.⁹ This technique involves etching away the sacrificial AlAs layer in order to release the heterostructures from the substrate. TEM observation was on a JEOL 2000FX operated at 200 kV.

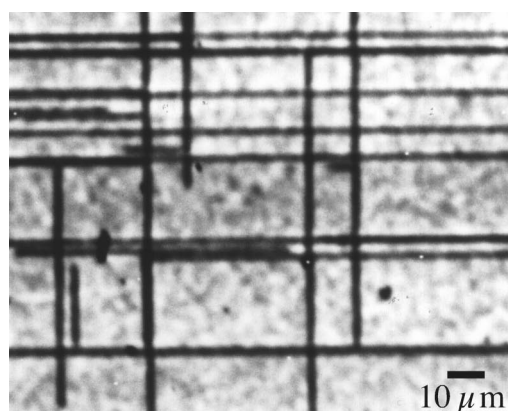
III. RESULTS

The CL images in Fig. 1 show the changes of dislocation configurations in a GaAs/In_{0.15}Ga_{0.85}As (25 nm)/GaAs specimen caused by thermal processing. The as-grown network of misfit dislocations [Fig. 1(a)] is unchanged by thermal processing at temperatures up to 1020 K, [Fig. 1(b)]. However, when the processing temperature reached 1040 K a large number of new, virtually straight, dislocations appeared [Fig. 1(c)]. The new dislocations form a network at 45° to the original network of misfit dislocations. No new dislocations were formed parallel to the original network.

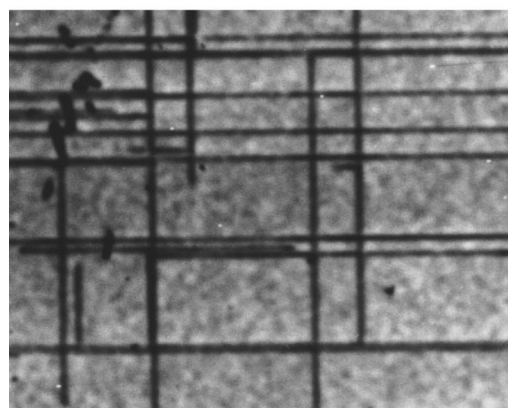
Figure 2 is a TEM plan-view of the 60° dislocations in the as-grown GaAs/In_{0.15}Ga_{0.85}As (25 nm)/GaAs structure. These misfit dislocations are formed at the strained-layer interfaces along the intersections of {111} slip planes and (001) interfaces, i.e., in <110> directions. The Burgers vectors of these dislocations are $a/2\langle 101 \rangle$, inclined at 45° to (001) and at 60° to their line directions.⁴

Figure 3 shows TEM images of dislocations in the same type of heterostructure after thermal processing at 1040 K. The dislocations in <110> directions, e.g., *M1* and *M2*, are 60° ones that pre-existed in the as-grown structure. The dislocation lines which are at 45° to the original 60° dislocations, such as *E1* and *E3*, are newly formed. These new dislocations are all in <100> directions. All dislocations lying in [010] directions, e.g., *E3*, are invisible in Fig. 3(c) when viewed using $\mathbf{g}=[040]$. From the criterion of $\mathbf{g}\cdot\mathbf{b}=0$, the invisibility of these dislocations shows that their Burgers vectors must lie in (010) planes and that they are therefore pure edge. Similarly, dislocations lying in [100] directions are also of edge type because they are invisible in Fig. 3(b) when viewed using $\mathbf{g}=[400]$, showing their Burgers vectors to lie in (100) planes.

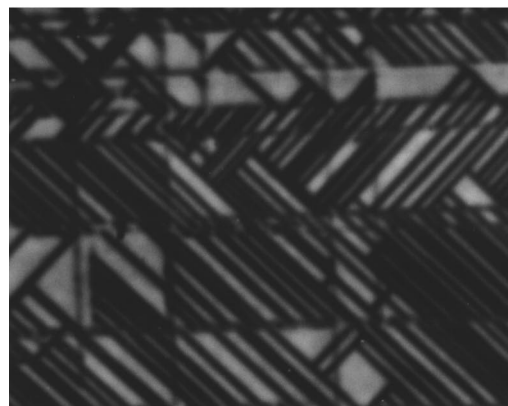
All of the newly formed dislocations are in pairs protruding from the original 60° dislocations. They are extensions of the original dislocations; there are no breaks. In Fig. 3(a), two pairs of dislocations, *E1* and *E2*, come from *c* and *d* respectively on the dislocation *M4*. Figure 3(c) shows that dislocation segment *M4* is diverted at *c* and *d* while dislocation segment *M1* is continuous at *a*. Thus *E1* and *E2* have been formed by extension of *M4*, not of *M1*. It can be seen from Fig. 3(b) that the pairs *E1* and *E2* interact with dislocation *M1* at *a*. Similarly, three pairs come from the line *M2*



(a)



(b)



(c)

FIG. 1. CL images of misfit dislocations in GaAs/In_{0.15}Ga_{0.85}As (25 nm)/GaAs: (a) original configuration, (b) after 300 s at 1020 K, (c) after 300 s at 1040 K.

and have been stopped by the newly formed dislocation pair *E1* as can be seen in Figs. 3(a) and 3(c).

So it is clear that all of the newly formed dislocations come from the pre-existing 60° dislocations. Some of them end at the pre-existing 60° dislocations, while others end at other newly formed dislocations. The newly formed dislocations must therefore lie in the interfaces, i.e., they are misfit dislocations.

Another feature of the newly formed dislocations is that all dislocation pairs generated from the same 60° dislocation

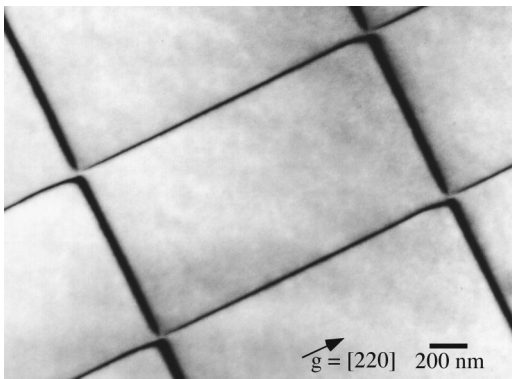


FIG. 2. 60° misfit dislocations in as-grown GaAs/In_{0.15}Ga_{0.85}As (25 nm)/GaAs (TEM bright field image).

line are oriented in the same direction. *M2* and *M3* can be regarded as one dislocation line; the pair *E3* can be identified as coming from *M2* but the pair *E4* do not come from *M3*. If the pair *E4* had come from the line *M3*, it would be invisible in Fig. 3(b) like *E3*, and there would be a break at *h* like that at *b*. The distortion of dislocation *M3* at *h* is further evidence that the pair *E4* did not come from the line *M3* but have interacted with it.

Figure 4 shows the effects of thermal processing at the same temperature (1040 K) on specimens with a larger indium concentration, viz. $x=0.2$. Similar analysis shows the newly formed dislocations to be oriented in [100] or [010] directions, while the original 60° dislocations lie in [110] or [110] directions.

The dislocation density for each specimen was estimated by averaging the dislocation line length per unit volume over a series of adjacent regions. The total dislocation densities increased during thermal processing from 1.5×10^6 to $6.5 \times 10^6 \text{ cm}^{-2}$ for $x=0.15$, and from 2.5×10^6 to $2 \times 10^7 \text{ cm}^{-2}$ for $x=0.20$.

IV. DISCUSSION

A. Relaxation by 60° and 90° misfit dislocations

The strain energy per unit volume, E_ϵ , in a strained layer is

$$E_\epsilon = 2G \left(\frac{1+\nu}{1-\nu} \right) \epsilon^2, \quad (1)$$

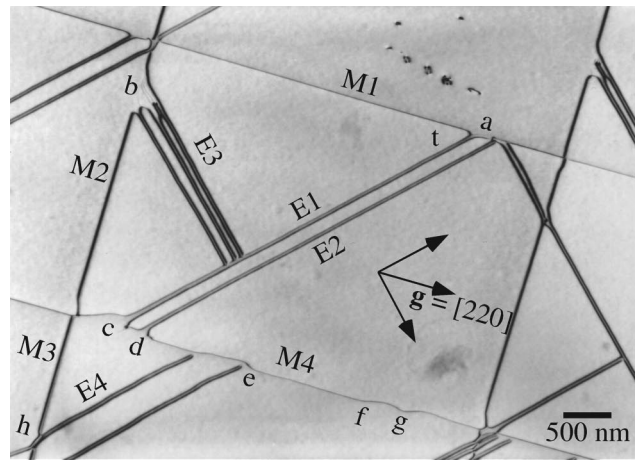
where ϵ is the strain, G is the shear modulus, and ν is Poisson's ratio. In a partially relaxed strained layer,

$$\epsilon = \epsilon_0 - \epsilon_r, \quad (2)$$

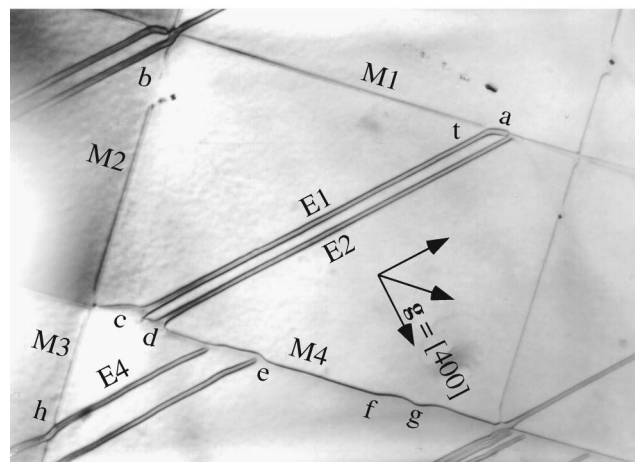
where ϵ_0 is the strain before relaxation and ϵ_r is the strain relieved by the misfit dislocations. The self-energy per unit volume, E_d , associated with the formation of a square array of dislocations per unit volume is given by^{7,10}

$$E_d = \frac{\rho G b_e^2}{4\pi(1-\nu)} \left[\ln \left(\frac{2\alpha h}{b} \right) - \frac{\cos 2\theta}{2} \right] + \frac{\rho G b_s^2}{4\pi} \ln \left(\frac{2\alpha h}{b} \right), \quad (3)$$

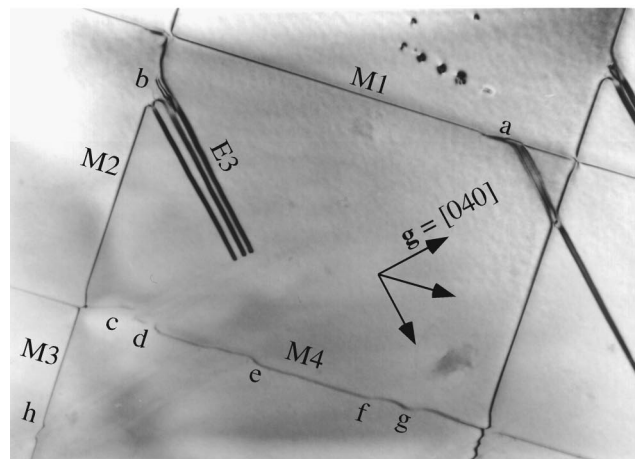
where α is the core parameter, b_e is the edge component and b_s is the screw component of the Burgers vector, θ is the



(a)



(b)



(c)

FIG. 3. Misfit dislocations in GaAs/In_{0.15}Ga_{0.85}As (25 nm)/GaAs after thermal processing at 1040 K (TEM bright field images).

angle between the Burgers vector and the normal to the surface, ρ is the linear misfit dislocation density, and h is the thickness of the strained layer. Thus the total energy, E , per unit volume is

$$E = E_\epsilon + E_d. \quad (4)$$

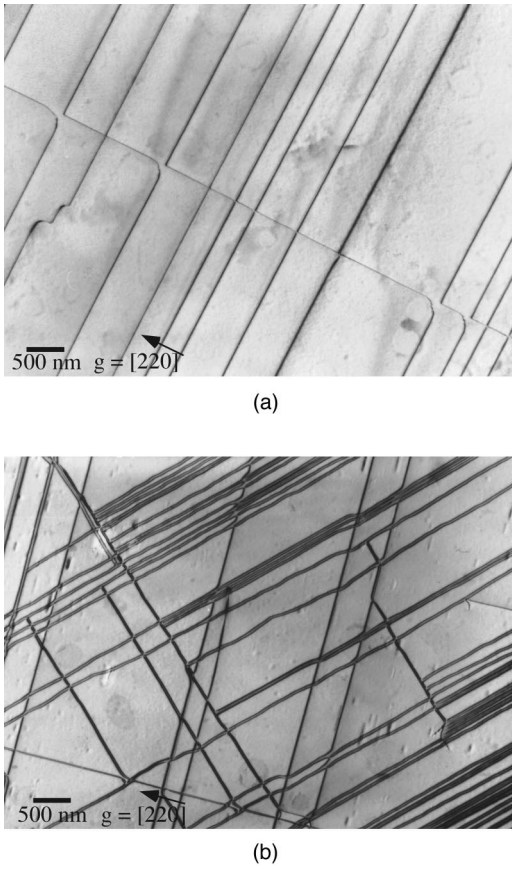


FIG. 4. Misfit dislocations in GaAs/In_{0.2}Ga_{0.8}As (20 nm)/GaAs: (a) 60° dislocations in the as-grown specimen, (b) after thermal processing at 1040 K.

Both the self-energy and strain energy terms are dependent on dislocation orientation. 60° misfit dislocations lie in $\langle 110 \rangle$ directions with $\mathbf{b} = a/2\langle 101 \rangle$, whereas the observed 90° (i.e., edge) dislocations lie in $\langle 010 \rangle$ directions with $\mathbf{b} = a/2\langle 101 \rangle$. For 60° dislocations, $b_e = (\sqrt{3}/2)b$ and $b_s = b/2$ while for 90° dislocations, $b_e = b$ and $b_s = 0$. As θ is 45° in each case, different values of E_d , referred to here as E_{d60° and E_{d90° respectively, can be calculated from Eq. (2) for these two types of misfit dislocations:

$$E_{d60^\circ} = \frac{\rho G b^2 (4-\nu)}{16\pi(1-\nu)} \ln\left(\frac{2\alpha h}{b}\right) \quad (5)$$

and

$$E_{d90^\circ} = \frac{\rho G b^2}{4\pi(1-\nu)} \ln\left(\frac{2\alpha h}{b}\right). \quad (6)$$

These expressions show that the self-energy per unit volume is greater for a network of edge-type dislocations than for 60° dislocations by a factor of $4/(4-\nu)$ for the same linear density of misfit dislocations. However, ϵ_r is greater by a factor of $\sqrt{2}$ for the edge-type dislocations⁷ and therefore, the increased value of E_d for these dislocations is counterbalanced by a reduced E_ϵ . Thus although each individual 90° misfit dislocation relieves more strain than a 60° one, initial strain relief occurs by the formation of an array of 60°

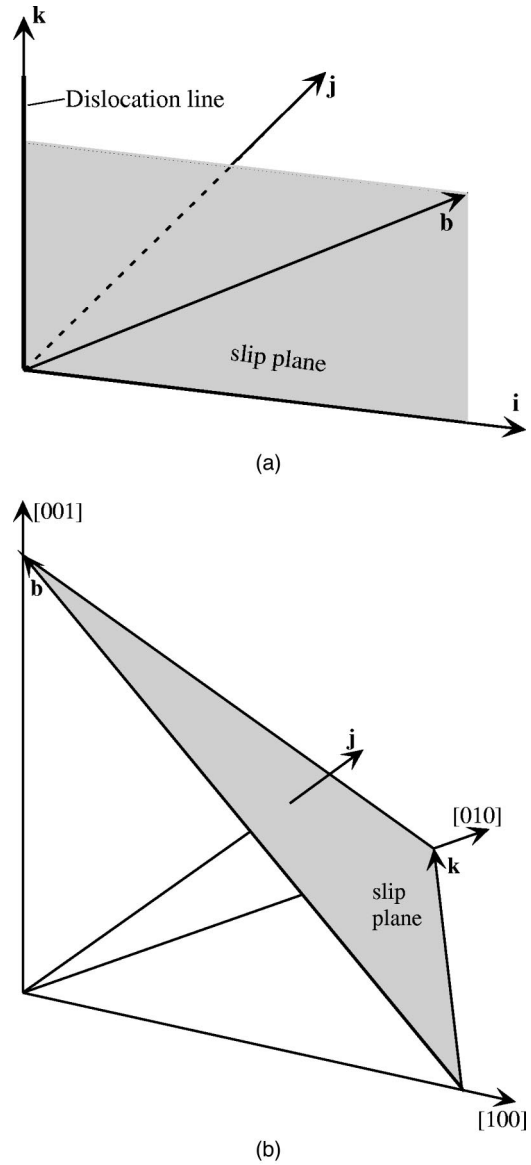


FIG. 5. 60° dislocation and its Burgers vector.

misfit dislocations. The subsequent formation of 90° misfit dislocations serves to lower the overall energy of the system by relieving some of the residual strain.

B. Effects of misfit stresses on 60° dislocations

The misfit accommodated by misfit dislocations with the geometry shown in Fig. 2 is

$$\delta = b/2d, \quad (7)$$

where d is the average separation of dislocations in the same interface. In GaAs/In_{0.15}Ga_{0.85}As/GaAs, d was measured as $\sim 1 \mu\text{m}$ and thus $\delta \approx 10^{-4}$. As this value for δ is less than 2% of the lattice misfit, there remains a driving force for the introduction of further misfit dislocations.¹¹

Only the edge component of the Burgers vectors of a misfit dislocation relieves misfit strain. Therefore the relaxation of misfit strain by the introduction of 60° misfit dislocations can be regarded as an imperfect process. Figure 5(a)

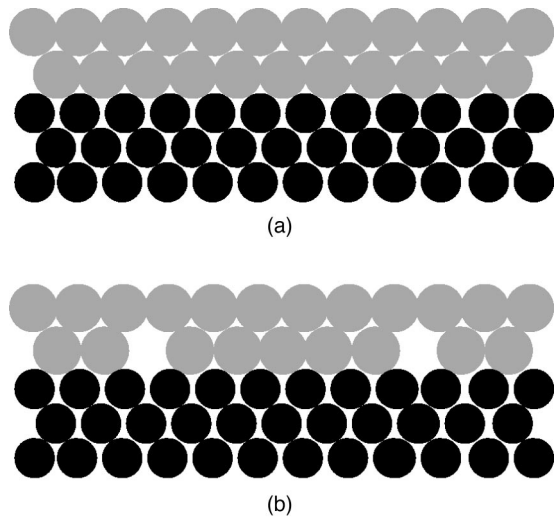


FIG. 6. Interfaces in a compressive strained-layer system: (a) coherent; (b) decorated with vacancies.

shows a 60° dislocation line parallel to the k axis, with a slip plane perpendicular to the j axis. The Burgers vector \mathbf{b} of the dislocation can be written as

$$\mathbf{b} = b_i \mathbf{i} + b_k \mathbf{k}, \quad (8)$$

where b_i and b_k are the edge and screw components of the Burgers vector and \mathbf{i} , \mathbf{j} , and \mathbf{k} are unit vectors in the i , j and k directions. The misfit shear stresses τ_{ik} and τ_{jk} exert a force on the screw component of the dislocation, and τ_{ii} and τ_{ij} exert a force on the edge component. The stresses τ_{jj} and τ_{kk} do no work and produce no force on the dislocation. The total force \mathbf{F} exerted on a unit length of the dislocation is^{12,13}

$$\mathbf{F} = -(\tau_{ij}b_i + \tau_{jk}b_k)\mathbf{i} + (\tau_{ii}b_i + \tau_{ik}b_k)\mathbf{j}. \quad (9)$$

The stresses τ_{jk} and τ_{ij} act on the dislocation in its slip plane while the stresses τ_{ik} and τ_{ii} act perpendicular to the slip plane.

For 60° dislocations in a zincblende structure, \mathbf{j} is the $\langle 111 \rangle$ direction normal to the slip plane given by $\mathbf{j} = \mathbf{k} \times \mathbf{b}$ [Fig. 5(b)]. The component of \mathbf{F} parallel to \mathbf{j} , F_j , acts on 60° dislocations along the $\langle 001 \rangle$ heterostructure interface in $\langle 110 \rangle$ directions, i.e., perpendicular to the dislocation lines. When climb processes are active, this force tends to move these dislocations away from their slip planes along the heterostructure interface, resulting in the emergence of edge dislocations on 60° misfit dislocations.

C. Vacancies as strain relievers and vacancy-producing jogs

Vacancies can be created at strained layer interfaces, emphasizing the periodic structure at the interface¹⁴ as shown in Fig. 6. Misfit stresses serve to move the vacancies along the interface to the most highly distorted sites, the most important of which are dislocations. Their motion is such that they continue to reflect the periodicity of the interfacial structure.

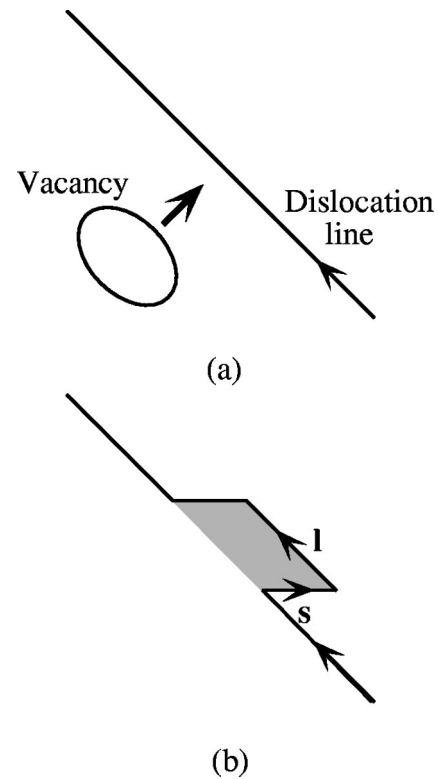


FIG. 7. Jog formation: (a) a vacancy or cluster of vacancies approaches a dislocation; (b) a jog is formed on the dislocation line.

Hopgood¹⁵ has proposed that vacancies in a compressively strained $\text{In}_x\text{Ga}_{1-x}\text{As}$ layer can relieve the strain energy. The strain energy per unit volume relieved by a vacancy concentration C_v can be expressed as

$$\Delta Q_v = -4G \left(\frac{1+v}{1-v} \right) \left(\frac{x C_v \Delta d_v \Delta d_{\text{In}}}{d_{\text{GaAs}}^2} \right), \quad (10)$$

where d_{GaAs} is the lattice constant of GaAs, d_v is the lattice constant of a GaAs unit cell containing one vacancy, $\Delta d_{\text{In}} = d_{\text{InAs}} - d_{\text{GaAs}}$, and $\Delta d_v = d_v - d_{\text{GaAs}}$. Thus ΔQ_v is the difference in strain energy per unit volume between vacancy-free $\text{In}_x\text{Ga}_{1-x}\text{As}$ on a GaAs substrate and $\text{In}_x\text{Ga}_{1-x}\text{As}$ containing vacancies on a GaAs substrate. The minus sign on the right-hand side of the Eq. 12 indicates that the creation of vacancies decreases the strain energy.

At high temperature, thermal activation assists the formation and movement of vacancies, enabling pre-existing dislocations to climb from their slip planes along the interfaces. The distortion of the dislocation line $M4$ at point g and section $e-f$ in Fig. 3(a) is evidence of this. The vacancy movement results in a jog on the original dislocation line (Fig. 7). If a small segment \mathbf{l} of dislocation undergoes a small displacement \mathbf{s} , the local change in volume, ΔV , is

$$\Delta V = \mathbf{b} \cdot \mathbf{l} \times \mathbf{s} = \mathbf{b} \times \mathbf{l} \cdot \mathbf{s}, \quad (11)$$

since the two sides of the area element $\mathbf{l} \times \mathbf{s}$ are displaced by \mathbf{b} relative to each other during the movement. The slip plane of the element is by definition perpendicular to $\mathbf{b} \times \mathbf{l}$. When either \mathbf{s} is perpendicular to $\mathbf{b} \times \mathbf{l}$ or $\mathbf{b} \times \mathbf{l} = 0$, so the element is pure screw, ΔV is zero. Otherwise, volume is not conserved ($\Delta V \neq 0$) and the motion is climb. For a 60° dislocation

$\mathbf{b} \times \mathbf{l} \neq 0$, and any movement away from its slip plane will produce an \mathbf{s} which cannot be perpendicular to $\mathbf{b} \times \mathbf{l}$. Therefore, the movement of 60° dislocations in any direction on the (001) interface plane is nonconservative. This is the mechanism for the formation of vacancy-producing jogs on a 60° dislocation. One of the most important processes of their formation is the absorption and emission of vacancies, i.e., jogs are sources and sinks for vacancies.^{16,17} The jogs will move away from the 60° dislocations under the effects of misfit stresses. A moving jog will trail a dislocation dipole and a string of vacancies.^{12,13,18}

As the jog moves through the lattice, the dislocation dipole trailed by it becomes longer until stopped by another dislocation. Because the jog is merely a segment of the dislocation itself and has the same Burgers vector as the remainder of the dislocation, any jogs on the pre-existing 60° dislocations must have a Burgers vector of $a/2\langle 101 \rangle$. As they lie in (001) planes and they are formed by climb, they must be pure edge type lying in $\langle 010 \rangle$ directions. Subsequent climb of those new edge dislocation segments must continue along (001) in the direction normal to their Burgers vectors. Thus, all these new edge dislocations are observed to grow in the same direction, at 45° to the pre-existing 60° dislocations. Motion in any other directions is inhibited by the high Peierls barrier. This may explain why bowing out of the point g and the section $e-f$ on dislocation line $M4$ in Fig. 3(a) could not develop further to form jogs or dislocation dipoles in other directions.

V. CONCLUSIONS

Pure edge-type misfit dislocations have been found to be introduced into GaAs/In_{0.15}Ga_{0.85}As/GaAs and GaAs/In_{0.20}Ga_{0.80}As/GaAs strained-layer heterostructures during thermal processing at 1040 K for up to 300 s. They form new orthogonal arrays of dislocations in addition to the pre-existing 60° dislocation network. In this way, the relaxed strained-layer structure is relaxed further. No new 60° dislocations are introduced during thermal processing.

60° dislocations are introduced during specimen growth either by nucleation on threading dislocations as in the M-B model, or by a different mechanism which dominates the global relation of the structure.⁹ They form a metastable orthogonal network. No further 60° misfit dislocations appear, even during thermal processing, because the misfit stress is reduced and the nucleation sites exhausted. Misfit stresses

remain in these as-grown structures which have been partially relaxed by 60° misfit dislocations. These stresses act as a driving force for the growth of new 90° edge misfit dislocations from the existing 60° misfit dislocations.

Thermal processing enables edge dislocations to grow by climb from the existing 60° misfit dislocations, thereby relieving more of the remaining strain. It is proposed that these edge dislocations are produced by vacancy-producing jogs protruding from pre-existing 60° dislocations. The jogs move out from the original dislocations by climb, trailing dislocation dipoles behind. The resultant dislocations have Burgers vectors of $a/2\langle 101 \rangle$ perpendicular to their $\langle 010 \rangle$ directions. Thus, two distinct mechanisms control the introduction of 60° and 90° misfit dislocations.

ACKNOWLEDGMENTS

Financial support from the Open University Research Committee is acknowledged. The authors are grateful to N. Williams for technical support.

- ¹J. W. Matthews and A. E. Blakeslee, *J. Cryst. Growth* **27**, 118 (1974).
- ²R. Hull and E. A. Stach, *Curr. Opin. Solid State Mater. Sci.* **1**, 1 (1997).
- ³E. A. Fitzgerald, *Mater. Sci. Rep.* **7**, 87 (1991).
- ⁴J. W. Matthews, A. E. Blakeslee, and S. Mader, *Thin Solid Films* **33**, 253 (1976).
- ⁵W. Hagen and H. Strunk, *Appl. Phys.* **17**, 85 (1978).
- ⁶L. B. Freund, *J. Mech. Phys. Solids* **38**, 657 (1990).
- ⁷R. Beanland, M. A. Lourenco, and K. P. Homewood, in *Microscopy of Semiconducting Materials 1997*, edited by A. G. Cullis and J. L. Hutchison (IOP, Bristol, 1997), p. 145.
- ⁸X. W. Liu and A. A. Hopgood, *Microscopy of Semiconducting Materials 1999*, edited by A. G. Cullis and R. Beanland (IOP, Bristol, 1999), p. 295.
- ⁹X. W. Liu, A. A. Hopgood, B. F. Usher, H. Wang and N. S. Braithwaite, *Semicond. Sci. Technol.* **14**, 1154 (1999).
- ¹⁰L. B. Freund, *J. Mech. Phys. Solids* **38**, 657 (1990).
- ¹¹V. Drigo, A. Aydinli, A. Carnera, F. Genova, C. Rigo, C. Ferrari, P. Franzosi, and G. Salviati, *J. Appl. Phys.* **66**, 1975 (1989).
- ¹²D. Hull and D. J. Bacon, *Introduction to Dislocations*, 3rd ed. (Pergamon, New York, 1984).
- ¹³J. Weertman and J. R. Weertman, *Elementary Dislocation Theory* (Oxford University Press, New York, 1992).
- ¹⁴J. W. Matthews, *Dislocations in Solids* (North-Holland, Amsterdam, 1979).
- ¹⁵A. A. Hopgood, *J. Appl. Phys.* **76**, 4068 (1994).
- ¹⁶F. R. N. Nabarro, *Theory of Crystal Dislocations* (Oxford University Press, New York, 1967).
- ¹⁷Kovacs and L. Zsoldos, *Dislocations and Plastic Deformation* (Pergamon, New York, 1973).
- ¹⁸J. P. Hirth and J. Lothe, *Theory of Dislocations* (McGraw-Hill, New York, 1968).